DOI: 10.61782/fa.2025.0956

FORUM ACUSTICUM EURONOISE 2025

VIBRO-ACOUSTIC STUDY OF A SMALL GLASS WALLED FISH TANK: AN EXPERIMENTAL AND THEORETICAL APPROACH

Naeem Ullah[1*] **Jesús Carbajo San Martin**[1] **Pedro Poveda Martinez**[1]
Jaime Ramis Soriano[1]
[1] Department of Physics, Systems Engineering, and Signal Theory, University of Alicante, Spain

ABSTRACT

Acoustic experiments in small water tanks, which study the behavior, auditory limitations, or negative effects of sound on marine animals, are very common. However, such tanks differ significantly from the animals' natural environments. While the natural environment is nearly an acoustic free field, tanks exhibit a reverberant field characterized by acoustic eigenmodes and the bending modes of the tank walls, which can significantly affect the field inside the tank depending on the wall properties. This study aims to investigate the acoustic field within a small glass-walled fish tank by examining the vibroacoustic behavior of its walls. Acoustic pressure measurements inside the tank are made using a hydrophone mounted on a robot, and acceleration measurements on the walls are made with an accelerometer. The experimental results demonstrate that wall bending modes can notably influence the tank's internal acoustic field. The results from the experimental work are compared with theoretical predictions to provide a broader view of the acoustic field inside the tank.

Keywords: *underwater acoustics, vibro-acoustics, fish tanks*

1. INTRODUCTION

Aquatic animals play a crucial role in human life by maintaining ecological balance, serving as a food source, boosting economies, advancing medical research, and enriching cultural traditions [1-3]. These contributions from aquatic animals make them very important and that is why different aspects of their lives are studied in great details and efforts are made to preserve them from different threats they are posed to. Among these studies acoustic studies on these animals are also common. The acoustic studies carried out on these animals focus on various aspects such as animal behavior [4], hearing capabilities [5], noise impact [6], and communication [7].

Most of the acoustic studies are carried out in small tanks that offer a controlled environment during the experiment and are more convenient. However, the acoustic field inside these tanks could be considerably different than the actual environment of the animal, depending on different specifications of the tank. This means that the tank has a different SPL distribution with altered dynamic range as compared to the actual environment, as well as the directivity of the field is also changed in the tank, attributed to the various properties of the tank. These changes are dominant in frequencies at the acoustic modes of the tank as well as the bending vibration modes of the walls. This may result in some uncertainties in the results and conclusions of these experiments, for instance the sound recorded from an animal in a tank may appear distorted compared to recordings made in situ [8-9], attributed to all or some of these aspects of the tanks.

The acoustic behavior and prediction of small tanks has been widely studied [10-12]. These kinds of works utilize experimental, theoretical, or a combination of both approaches to analyze and predict the acoustic fields within the tanks. Theoretical models are often developed to closely match experimental results by incorporating some properties such as the flexibility, losses or damping characteristics of the tank walls. Whereas most of the experimental works are constrained by relying primarily on sound pressure measurements at limited locations, which can limit the details of the acoustic field and hence the comprehensiveness of the findings. Expanding such studies to include broader measurement techniques with greater spatial resolutions could enhance our understanding of the complex acoustic dynamics within these structures.

[*] ***Corresponding author***: naeem.ullah@ua.es.

This work provides a detailed account of the acoustic field inside small glass walled tanks, taking into account the vibroacoustic behavior of the walls. An automated robotic system is implemented to measure the sound pressure inside the tank with greater spatial accuracy and resolution. Vibration measurements on two of the adjacent walls are made with high resolution using an accelerometer. The sound pressure inside and tank and acceleration on the walls are analyzed to study the vibroacoustic effects of the walls. The results show that the acoustic field induces vibrations in the walls that significantly affect the sound field inside the tank close to the walls, especially at frequencies at its bending modes. The vibroacoustic effects of the walls are more dominant in the lower frequencies i.e. below 1 kHz for the system considered.

2. MATERIAL AND METHODS

2.1 Fish tank setup

The fish tank setup used in the experiment is shown in Fig. 1. The experiment is conducted in a quartz glass water tank with internal dimensions of 494 × 258 mm, wall height of 293 mm, and wall thickness of 2.98 mm. The tank is filled with water to a height of 200 mm. The perimeter of the base of the tank is supported by a small aluminum frame that prevents the bottom face of the tank from touching the ground allowing it to vibrate freely. The tank is made of connecting different plates of glass with the help of a special glue.

A sound source (TECTONIC TEAX19C01-8), a Distributed Mode Loudspeaker (DML) mounted on a circular plastic base with a diameter of 60 mm, is positioned inside the tank, at an approximate location of (33, 129, 100) mm. The source is supported inside the tank by a small rod mounted on a supporting structural frame. To measure the sound pressure inside the tank, a hydrophone (AQUARIAN AS-1) is mounted on a robotic system at a height of 100 mm from the bottom of the tank. The robot, equipped with two step motors controlled via Arduino, is a 2-DOF system that moves in the X and Y directions to enable automatic measurements of sound pressure in multiple predefined locations in the horizontal XY plane. To study the vibration behavior of the tank walls, caused by the sound source inside the tank, acceleration measurements are made with the help of an accelerometer (B&K Type-4517) on marked grids in two of the walls (YZ plane and XZ plane) as shown in Fig. 1.

An in-house-built application, developed using NI LabVIEW, is employed to control the robotic system and ensure the synchronized operation of the source and the hydrophone at each measuring location. During the acoustic measurements the robot moves to the defined locations one by one and when the system is stationary, an MLS signal is sent through a DAQ card (NI-USB X Series) to a sound amplifier (PASCO PI-9587C) which amplifies it and eventually feeds it to the sound source. At the same time as the sound source emits, the sound pressure at the hydrophone is recorded. The signal from the hydrophone goes to a phantom power supply (SHURE PS1A) from where it is sent to a conditioning amplifier (B&K NEXUS 2693—OS4-) then it finally goes to the same DAQ card. This data is then eventually stored on a computer. A block diagram of the process used in the emission and reception of the data is shown in Fig. 2.

Once the acoustic measurements are completed, acceleration measurements on the walls are made. To record the acceleration data at each location the same procedure is used as in pressure measurements, except the accelerometer being moved manually. The same sound source is used to emit the MLS signal, and the acceleration measurements are made simultaneously by the accelerometer. The signal from the accelerometer passes through the same devices as in the pressure measurement case except that the phantom power supply is not used, as shown in Fig. 2.

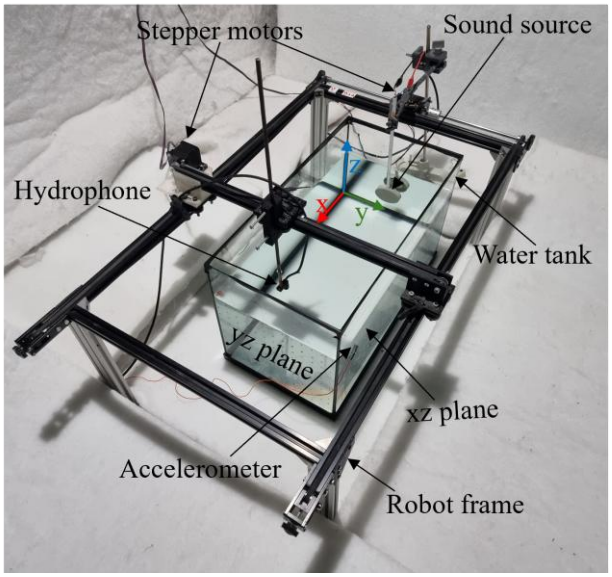

Figure 1. Fish tank with experimental setup and robot.

For each recording grid position in both the pressure and acceleration measurements, a 0.74-second MLS signal is

emitted from the sound source with six repetitions and recorded simultaneously with a sampling frequency of 44100 Hz at the hydrophone or accelerometer during their respective measurements. MLS signal is used because of its high signal to noise ratio (SNR) [13-14]. Later in the processing stage a cross correlation of the input MLS signal and recorded signal at each position is performed to calculate the impulse response. The middle impulse response is adopted to calculate the pressure and acceleration spectrums for their respective measurements. The spectrums are obtained by applying the Fast Fourier Transform (FFT) to the impulse response in MATLAB®.

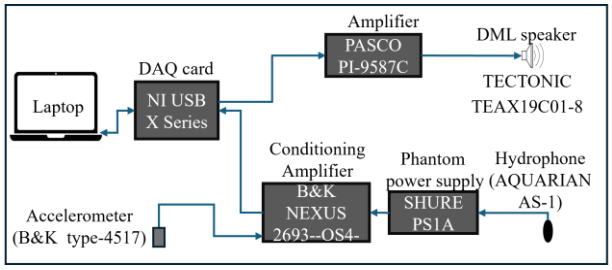

Figure 2. Block diagram of the process used in the emission and reception of the data.

2.2 Pressure measurements

The sound pressure measurements inside the tank are conducted by selecting rectangular grids of 252 points in a horizontal plane at a distance of 100 mm from the bottom of the tank. The grid in each horizontal plane consists of twenty-one recording points in the X direction spanning over a length of 370 mm with 18.5 mm resolution, and twelve recording points in the Y direction spanning over a length of 230 mm with 20.9 mm resolution. Along the X direction the starting point of the recordings is at X=115 mm due to limitation on the robot's motion posed by the sound source, shape of the robot and the frame holding the hydrophone which can result in collision of robot with the sound source support if the robot is moved further closer in the X direction. The end of the X recording points is nearly 485 mm. In the Y direction the starting and end points are approximately 14 mm and 244 mm, respectively. Consequently, part of the XY plane is not measured; however, it does not impact the accurate representation of the SPL fields and mode shapes.

2.3 Acceleration measurements

The acceleration measurements on the YZ and XZ walls are conducted by marking grids of 130 and 250 points on each of the walls, respectively. The YZ wall includes ten measurement points in the Z-direction and thirteen points in the Y-direction, while the XZ wall features ten points in the Z-direction and twenty-five points in the X-direction. The starting point location in the YZ plane is (Y, Z)=(9, 20) mm while the end point is (Y, Z)=(249, 200) mm, making the two opposite corners of the 130 points rectangular grid. Whereas in the XZ plane the starting and end points are (X, Z)=(7, 20) mm and (X, Z)=(487, 200) mm respectively, making the two opposite corners of the 250 points rectangular grid. The spatial resolution of measurements on both the walls is 20 mm.

3. NUMERICAL MODEL

In addition to the experimental measurements, a FEM numerical model is developed using COMSOL Multiphysics®. The model employs pressure acoustics and structural mechanics (Shell) studies combined by a Multiphysics interface in the frequency domain. A tank of the same dimensions and water height is developed as in the experiment. The sound source is designed as a cap-like structure with a diameter of 60 mm and edge length 10 mm. The source is positioned in approximately the same location and orientation inside the water medium, as in the experiments.

Approximate property values are assigned to the tank walls and water inside the tank. For water the speed of sound and density are adopted to be 1500 m/s and 1000 kg/m³, respectively. While for the glass medium the Young's modulus, density, Poisson's ratio, and loss factor are adopted to be 80 GPa, 2600 kg/m³, 0.15, and 0.002 respectively. The exact properties of the two media are unknown and the adopted values of properties lie within the range of the values generally shown by the two media. The tank is designed as a single body in contrast to the actual case where it is made by joining plates with glue. Results show that this choice does not considerably affect the acoustic modes inside the tank, though it affects the bending modes considerably.

The water surface is modeled as a null pressure [15] surface boundary condition. The perimeter of the bottom face of the tank is modeled with a fixed constraint condition, while the face itself is assigned an acoustic-structure boundary condition and is free to vibrate, accurately depicting the actual scenario. Parts of all the four walls in contact with water are treated with acoustic-structure boundary conditions, while the parts in contact with air are assumed to be in vacuum. The face of the cap-like sound source is assigned with an interior velocity condition with an

amplitude of 0.1 m/s, while the edges are treated as acoustic hard boundaries.
Simulations are conducted with a maximum frequency of 10000 Hz, with a frequency step of 2 Hz below 1 kHz and 5 Hz for higher frequencies. The COMSOL® numerical model is shown in Fig. 3.

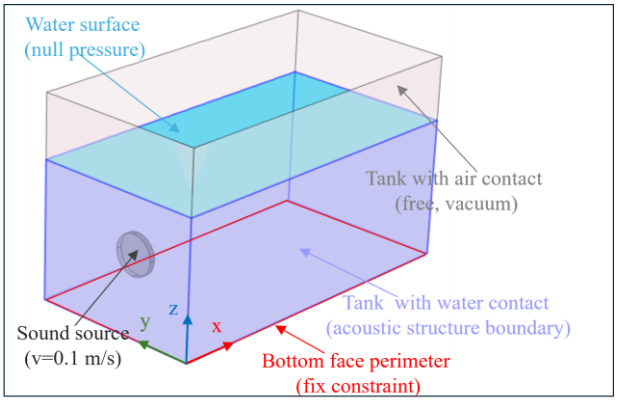

Figure 3. Developed numerical model in COMSOL® with boundary conditions.

The acoustic wavelength inside the water medium is greater than the bending-wave wavelength inside the walls for the frequency range of interest. A mesh size of seven elements per wavelength is adopted based on bending-wave for frequencies below 1 kHz while for higher frequencies it is based on the acoustic waves inside water. This mesh setup is selected because of time efficiency and the vibration behavior of the walls seems to be more dominant up to 1kHz. This choice of mesh for higher frequencies does not affect the overall response of the tank in terms of the acoustic modes inside the water except the bending behavior of the walls which again does not affect the overall pressure field inside the tank noticeably.

4. RESULTS AND DISCUSSION

Analyzing the sound pressure profile inside the tank and the acceleration profile of the walls reveal two types of modes: the bending eigenmodes and the acoustic eigenmodes. The bending eigenmodes correspond to the natural vibration modes of the tank structure, while the acoustic eigenmodes represent the acoustic modes occurring within the waterbody. Peaks related to the two modes are seen in both the pressure and acceleration spectrums.
The SPL profile in the horizontal plane inside the tank shows that higher SPL lobes occur due to the vibroacoustic behavior of the walls. Comparing the vibrations profile of the walls and SPL profile inside water confirms it. This is because the incident acoustic waves induce vibrations in the tank walls [16] which reradiate and contribute to the sound pressure inside the tank. These effects are more dominant at the bending eigenmodes. It can be noted that the acoustic eigenmodes also induce very clear and dominant vibrations in the walls.

4.1 Sound pressure level vs acceleration level spectrum

The mean acceleration spectrum of points on a horizontal line Z= 100 mm (same height as SPL plane) on the XZ wall and the mean SPL spectrum of points on a line Y=244 mm on the horizontal plane are shown in Fig. 4. Peaks related to the bending modes of the wall can be seen in the SPL spectrum while peaks corresponding to the acoustic modes can be seen in the acceleration spectrum. In the frequency range below the first acoustic mode, the contributions to SPL due to the vibroacoustic effects of the walls seem to be more dominant below 1 kHz as the SPL spectrum shows higher values in this frequency zone.

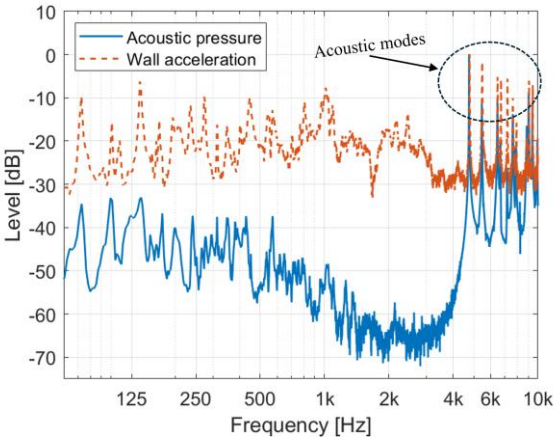

Figure 4. Mean sound pressure spectrum along a line in the horizontal plane and mean acceleration spectrum along a line on the XZ wall, from the experimental study. The two lines are next to each other in the corresponding planes. Levels are represented with respect to the values at the first acoustic mode (4752 Hz) of the respective data.

4.2 Eigenmode shapes

Results show that the bending mode produces an acoustic profile inside the tank, near the walls, with a shape similar to that of the bending mode. Meanwhile, the acoustic

modes inside the tank create a vibration profile on the walls, resembling the shapes of the acoustic modes.

4.2.1 Bending eigenmode shapes

The shapes of three bending eigenmodes along with the SPL profile inside the tank are shown in Fig. 5 for both the experimental (a1-c1) and numerical (a2-c2) works. The first two experimental modes at 71 Hz and 135 Hz are selected as they are very close to the important frequencies (63 Hz and 125 Hz) in acoustics studies. That first two modes (a, b) are related to the XZ wall while the last mode (c) is related to the YZ wall. The horizontal plane shows an SPL dynamic range (DR) of about 42 dB experimentally and about 48 dB numerically, at the three frequencies. It shows that the vibration modes of the wall produce considerable increase in SPL inside the horizontal plane close to the walls. Both the experimental and numerical figures display similar shapes; however, the numerical frequency values are significantly higher than those observed in the experimental work. This discrepancy may be attributed to uncertainties in the system properties adopted and the simplified single-body numerical model, which contrasts with the real tank constructed by glueing individual plates together. However, the higher frequency acoustics modes show better results.

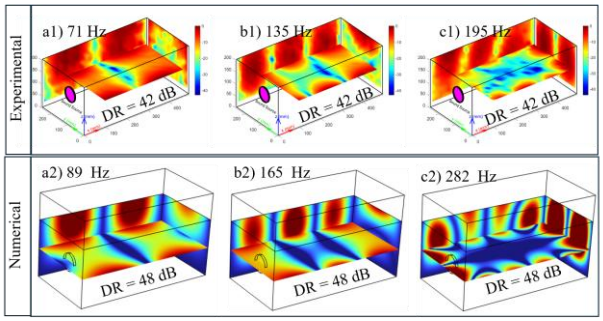

Figure 5. Three of the bending mode shapes of the tank walls from experimental (a1-c1) and numerical (a2-c2) works. The first two modes (a,b) are related to the XZ wall while and the third mode (c) is related to the YZ wall. The modes significantly contribute to SPL. Levels in each plane are calculated with respect to maximum value in each plane at each frequency. DR means dynamic range.

4.2.2 Acoustic eigenmode shapes

The shapes of three acoustic eigenmodes along with the acceleration profile on the walls are shown in Fig. 6 for both the experimental (a1-c1) and numerical (a2-c2) works. As the water surface is in contact with air it is a null pressure surface [15] so there is at least one Z pressure node in each acoustic mode. The 1st mode has Mx=0, My=0, and Mz =1, where Mi is the number of pressure nodes in the ith direction. The 2nd and the third modes are Mx=1, My=0, Mz=1 and Mx=2, My=0, Mz=1, respectively. It is seen that these acoustic modes induce vibrations of the same shapes in the walls. The numerical model shows the same shape SPL profile inside the tank; however, the vibration profile shows some difference compared to the experimental work, which once again could be attributed to the same discrepancies in the numerical model as well as the existence of background noises in the experimental case. Nonetheless, the error in the numerically calculated values for the first three acoustics modes lies within 2 %.

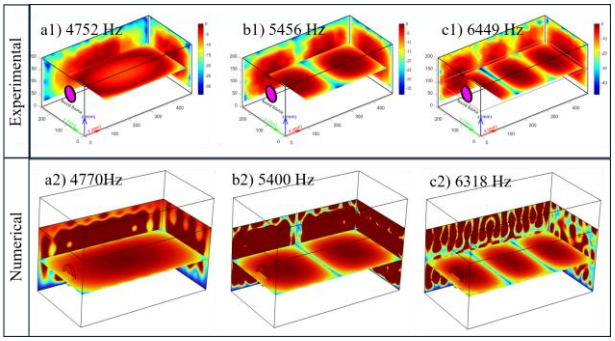

Figure 6. First three acoustic mode shapes inside the tank from experimental (a1-c1) and numerical (a2-c2) works. The acoustics modes induce vibrations of the same shapes in the walls. Levels in each plane are calculated with respect to maximum value in each plane at each frequency.

4.3 Higher acoustic modes: experimental vs numerical

The numerical values of the first seven acoustics modes lie with 3% of the experimental values. The first seven acoustic modes resulting from the experimental and numerical FEM model are shown in detail in Tab. 1. The numerical model shows greater accuracy (error below 1%) for modes that contain a pressure node in Y direction (My), as compared to modes with pressure nodes only in the X direction (Mx) (error above 3%).

Analysis of the numerical model shows that the acoustic modes change considerably with changing the boundary conditions of the tank walls and height of the water column. For instance, changing the bottom face boundary conditions from free and acoustic structure boundary condition to rigid condition reduces the first mode value by almost 1000 Hz, whereas decreasing the water height considerably increases the acoustic eigenmode frequencies and vice versa. The experimental calculations were repeated the next day, and it showed that the first acoustic mode had increased by almost 20 Hz the next day, this is due to the slight decrease in water height that occurred due to evaporation. So, one of the reasons for the error could be the fact that the height of water in the experiment was not exactly 200 mm. This change in the acoustic eigen frequencies with height can also be simulated in the numerical model. The numerical model also shows that changing the values of mechanical properties of the tank does not show considerable change in acoustics mode frequencies, hence their uncertainty contributes the least to the error.

Table 1. Comparison of the first seven acoustic modes form experiment and numerical model. Mz values are based on numerical results.

Mx	My	Mz	Experimental	Numerical	% error
0	0	1	4752 Hz	4770 Hz	0.38
1	0	1	5456 Hz	5400 Hz	1.03
2	0	1	6449 Hz	6318 Hz	2.03
0	1	1	6682 Hz	6726 Hz	0.66
1	1	1	7162 Hz	7137 Hz	0.35
3	0	1	7628 Hz	7428 Hz	2.62
2	1	1	7903 Hz	7917 Hz	0.18

5. CONCLUSIONS

Preliminary experimental results show that the vibroacoustic effects of the walls influence the SPL inside the tank to a considerable extent, especially in the low frequency. Hence the position of hydrophone during acoustic measurements must be chosen with care depending on the specific experiment and frequencies of interest.
Accelerometer measurements on the walls, instead of pressure measurements inside the tank could be used to measure the frequencies related to the acoustic modes of similar tanks (with single layered walls), as seen in this work.
The numerical model shows adequate results in terms of the high frequency acoustic response and modes and hence could be used to predict the tank's response using reasonable properties for water and tank walls even if they are not exactly known. To achieve more accurate results, the numerical model needs refinement, particularly by incorporating more precise conditions at the wall joints which are glue connected glass walls.

6. ACKNOWLEDGMENTS

This publication is part of the project PID2021-127426OB-C22, funded by MCIN/AEI/10.13039/501100011033 and by the European Union "NextGenerationEU"/PRTR," with the reference stated in the grant resolution. MCIN is the acronym for the Ministry of Science and Innovation; AEI is the acronym for the State Research Agency; 10.13039/501100011033 is the DOI (Digital Object Identifier) of the Agency; and PRTR is the acronym for the Recovery, Transformation, and Resilience Plan.

7. REFERENCES

[1] J. D. Olden, J. R. S. Vitule, J. Cucherousset, and M. J. Kennard, "There's more to fish than just food: Exploring the diverse ways that fish contribute to human society," Fish., vol. 45, no. 9, pp. 453–464, 2020.

[2] J. H. Harris, "The use of fish in ecological assessments," Aust. J. Ecol., vol. 20, pp. 65–80, 1995.

[3] A. J. Dyck and U. R. Sumaila, "Economic impact of ocean fish populations in the global fishery," *J. Bioecon*, vol. 12, pp. 227–243, 2010.

[4] E. M. Panova, R. A. Belikov, A. V. Agafonov, et al., "The relationship between the behavioral activity and the underwater vocalization of the beluga whale (Delphinapterus leucas)," Oceanol., vol. 52, pp. 79–87, 2012.

[5] R. A. Kastelein, R. van Schie, W. C. Verboom, and D. de Haan, "Underwater hearing sensitivity of a male and a female Steller sea lion (Eumetopias jubatus)," *J. Acoust. Soc. Am.*, vol. 118, no. 3, pp. 1820–1829, Sep. 2005.

[6] R. H. Pieniazek, M. F. Mickle, and D. M. Higgs, "Comparative analysis of noise effects on wild and captive freshwater fish behaviour," *Anim. Behav.*, vol. 168, pp. 129–135, 2020.

[7] C. Hyacinthe, J. Attia, and S. Rétaux, "Evolution of acoustic communication in blind cavefish," Nat. Commun., vol. 10, p. 4231, 2019.

[8] T. Akamatsu, T. Okumura, N. Novarini, and H. Y. Yan, "Empirical refinements applicable to the recording of fish sounds in small tanks," *J. Acoust. Soc. Am.*, vol. 112, no. 6, pp. 3073–3082, Dec. 2002.

[9] Y. Jézéquel, J. Bonnel, J. Coston-Guarini, and L. Chauvaud, "Revisiting the bioacoustics of European spiny lobsters Palinurus elephas: comparison of antennal rasps in tanks and in situ," *Mar. Ecol. Prog. Ser.*, vol. 615, pp. 143–157, 2019.

[10] P. A. Anderson, "Acoustic characterization of seahorse tank environments in public aquaria: A citizen science project," *Aquac. Eng.*, vol. 54, pp. 72–77, 2013.

[11] R. Tang, Y. Zhang, Q. Li, and D. Shang, "The investigation of the methods for predicting the sound field in a non-anechoic tank with elastic boundary," in *Proc. IEEE/OES China Ocean Acoustics Symp.*, (Harbin, China), pp. 000–111, 2016.

[12] A. Novak, M. Bruneau, and P. Lotton, "Small-sized rectangular liquid-filled acoustical tank excitation: A modal approach including leakage through the walls," *Acta Acust. united Acust.*, vol. 104, pp. 586–596, 2018.

[13] J. L. Nielsen, "Improvement of signal-to-noise ratio in long-term MLS measurements with high-level nonstationary disturbances," *J. Audio Eng. Soc.*, vol. 45, no. 12, pp. 1063–1066, 1997.

[14] M. Vorländer and M. Kob, "Practical aspects of MLS measurements in building acoustics," *Appl. Acoust.*, vol. 52, no. 314, pp. 239–258, 1997.

[15] C. Erbe, A. Duncan, and K. J. Vigness-Raposa, "*Introduction to sound propagation under water*," in *Exploring Animal Behavior Through Sound: Volume 1 Methods*, C. Erbe and J. A. Thomas, Eds. Springer, 2007.

[16] F. Fahy and P. Gardonio: *Sound and structural vibration: radiation, transmission and response*. Oxford: Academic Press (Elsevier), 2007.